189942: muscovite–biotite syenogranite, Lewis Range

(Lewis Granite, Granites–Tanami Orogen)

Location and sampling

LUCAS (SF 52-2), LEWIS (4657)
MGA Zone 52, 461965E 7774234N

Sampled on 6 June 2007

This sample was collected from an outcrop northeast of the Lewis Range, about 27 km south of the Tanami Road, 7.5 km north of Point Nelligan, and 4.0 km west of Schultz Cairn.

Tectonic unit/relations

The unit sampled is the Lewis Granite of the Granites–Tanami Orogen (Eacott and de Souza Kovacs, 2015). The Lewis Granite covers an area of about 9000 km^2 and consists of monzogranite and granodiorite, crosscut by rare pegmatite and aplite dykes (Bagas et al., 2010). The Lewis Granite is a composite intrusion, consisting of domains of low and moderate to high magnetization; the present sample is from a weakly magnetized phase. Weakly magnetized Lewis Granite, sampled about 35 km to the east-southeast, yielded a magmatic crystallization age of 1796 ± 24 Ma (GSWA 184811, Bagas et al., 2010). Another weakly magnetized granodiorite of the Lewis Granite, sampled about 13.5 km to the east-southeast, yielded a magmatic crystallization age of 1800 ± 15 Ma (GSWA 189936, Lu et al., 2018).

Petrographic description

The sample is a muscovite–biotite syenogranite, consisting of about 40–45% quartz, 30–35% K-feldspar, 15% plagioclase, 7% muscovite, 6% biotite, and minor tourmaline and apatite. Quartz is mostly anhedral, up to 4 mm in size, partly in graphic intergrowths with K-feldspar, and appears to be partially resorbed. K-feldspar (mainly orthoclase) is anhedral, up to 5 mm in size, and locally contains graphic quartz inclusions. Plagioclase is subhedral to euhedral, up to 3 mm long, and exhibits sericite alteration. Biotite is up to 2 mm long, and accompanied by irregular muscovite grains and yellow tourmaline up to 3 mm long. Weak sericite alteration in plagioclase, together with clay minerals, chlorite and possible K-feldspar in altered biotite, indicate low-temperature alteration.

Zircon morphology

Zircons isolated from this sample are pale brown to dark brown or opaque, and subhedral to euhedral. The crystals are up to 300 μm long, and equant to elongate, with aspect ratios up to 6:1. In cathodoluminescence (CL) images, most crystals consist of concentrically zoned cores surrounded by high-uranium, zoned, metamict rims. A CL image of representative zircons is shown in Figure 1.

Analytical details

This sample was analysed on 21 July 2008, using SHRIMP-A. Seven analyses of the Temora 2 standard obtained during the session indicated an external spot-to-spot (reproducibility) uncertainty of 0.50% (1σ), and a $^{238}U/^{206}Pb^*$ calibration uncertainty of 0.34% (1σ). Calibration uncertainties are included in the errors of $^{238}U/^{206}Pb^*$ ratios and dates listed in Table 1. Common-Pb corrections were applied to all analyses using contemporaneous isotopic compositions determined according to the model of Stacey and Kramers (1975).

Results

Sixteen analyses were obtained from 16 zircons. Zircon rims could not be analysed successfully, owing to their very high uranium and common Pb contents. Results are listed in Table 1 and shown in a concordia diagram (Fig. 2).

Interpretation

The analyses are concordant to strongly discordant (Fig. 2). Five analyses are >5% discordant. The dates obtained from these five analyses (Group D; Table 1) are unreliable, and are considered not to be geologically significant. The remaining 11 analyses can be divided into two groups, based on their $^{207}Pb^*/^{206}Pb^*$ ratios.

Group X comprises nine analyses of zircon cores (Table 1), which yield $^{207}Pb^*/^{206}Pb^*$ dates of 2692–1865 Ma.

Group P comprise two analyses of zircon cores (Table 1), which yield $^{207}Pb^*/^{206}Pb^*$ dates of 1747 and 1735 Ma.

The dates of 2692–1865 Ma for the nine analyses in Group X are interpreted as the ages of xenocrystic zircons. Although it remains a possibility that the c. 1865 Ma dates reflect magmatic crystallization, the dominance of zircons of this age in the Tanami Group host rocks, and the crystallization ages of 1800–1788 Ma obtained elsewhere for the Lewis Granite suggest that these are xenocrysts. The youngest date of 1865 ± 12 Ma (1σ) in Group X thus represents a maximum age for igneous crystallization of the syenogranite.

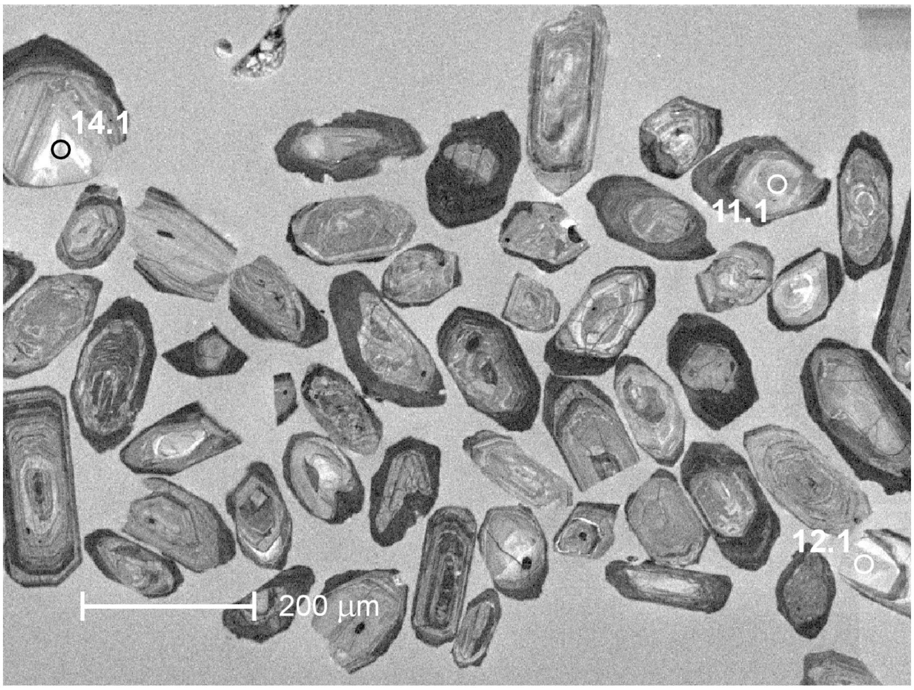

Figure 1. **Cathodoluminescence image of representative zircons from sample 189942: muscovite–biotite syenogranite, Lewis Range. Numbered circles indicate the approximate locations of analysis sites**

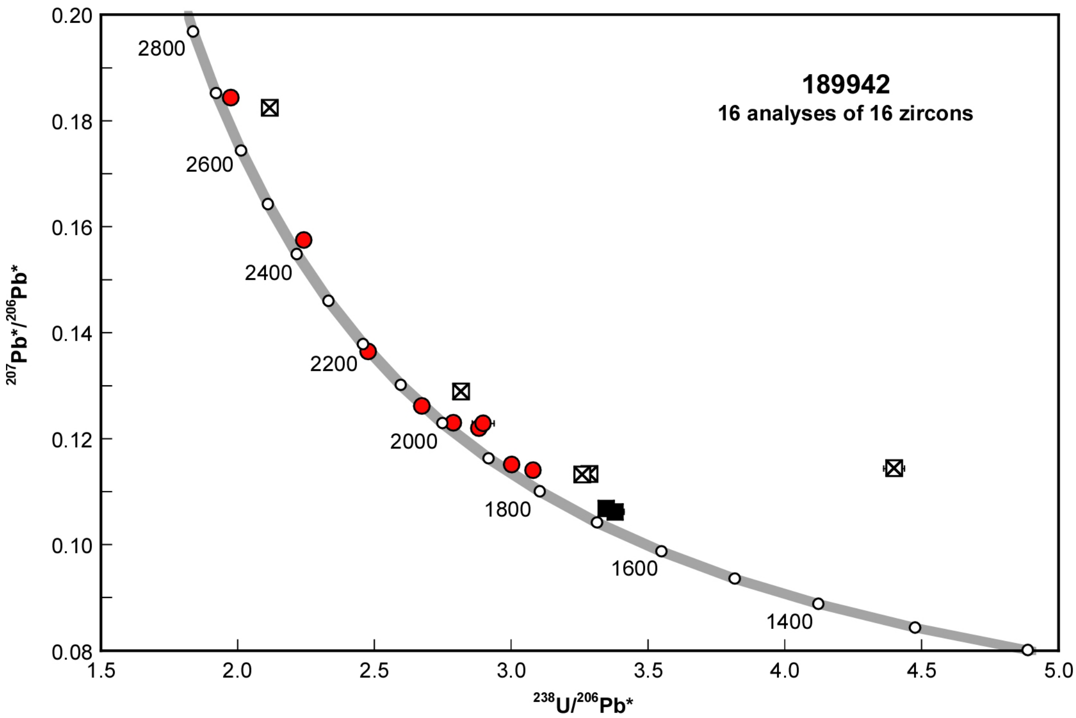

Figure 2. **U–Pb analytical data for zircons from sample 189942: muscovite–biotite syenogranite, Lewis Range. Red circles indicate Group X (xenocrystic zircons); Black squares indicate Group P (radiogenic Pb loss); crossed squares indicate Group D (discordance >5%)**

Table 1. Ion microprobe analytical results for zircons from sample 189942: muscovite-biotite syenogranite, Lewis Range

Group ID	Spot no.	Grain. spot	^{238}U (ppm)	^{232}Th (ppm)	$\frac{^{232}Th}{^{238}U}$	$f204$ (%)	$^{238}U/^{206}Pb$	$\pm 1\sigma$	$^{207}Pb/^{206}Pb$	$\pm 1\sigma$	$^{238}U/^{206}Pb^*$	$\pm 1\sigma$	$^{207}Pb^*/^{206}Pb^*$	$\pm 1\sigma$	$^{238}U/^{206}Pb^*$ date (Ma)	$\pm 1\sigma$	$^{207}Pb^*/^{206}Pb^*$ date (Ma)	$\pm 1\sigma$	Disc. (%)
X	2	2.1	218	57	0.26	0.222	3.073	0.026	0.11598	0.00062	3.080	0.026	0.11404	0.00076	1813	13	1865	12	2.8
X	11	11.1	284	81	0.28	0.097	2.997	0.025	0.11603	0.00058	3.000	0.025	0.11518	0.00064	1855	13	1883	10	1.5
X	10	10.1	573	226	0.39	0.012	2.882	0.021	0.12212	0.00040	2.883	0.021	0.12201	0.00040	1920	12	1986	6	3.3
X	12	12.1	187	50	0.26	0.130	2.894	0.040	0.12400	0.00074	2.897	0.040	0.12286	0.00084	1911	23	1998	12	4.3
X	5	5.1	115	90	0.78	0.057	2.788	0.027	0.12351	0.00086	2.789	0.027	0.12301	0.00091	1975	17	2000	13	1.3
X	13	13.1	285	110	0.39	0.139	2.671	0.022	0.12740	0.00057	2.675	0.022	0.12618	0.00065	2047	14	2045	9	-0.1
X	3	3.1	172	83	0.48	0.021	2.477	0.022	0.13662	0.00069	2.477	0.022	0.13643	0.00070	2186	16	2182	9	-0.2
X	1	1.1	371	100	0.27	0.113	2.239	0.023	0.15850	0.00058	2.242	0.023	0.15749	0.00062	2378	21	2429	7	2.1
X	14	14.1	102	53	0.52	0.120	1.974	0.021	0.18543	0.00110	1.976	0.021	0.18436	0.00117	2639	23	2692	10	2.0
P	9	9.1	160	524	3.28	0.507	3.363	0.032	0.11060	0.00081	3.380	0.032	0.10620	0.00120	1671	14	1735	21	3.7
P	8	8.1	304	304	1.00	0.011	3.346	0.027	0.10695	0.00057	3.347	0.027	0.10686	0.00058	1685	12	1747	10	3.5
D	7	7.1	412	102	0.25	0.225	3.263	0.025	0.11520	0.00050	3.270	0.025	0.11323	0.00061	1720	11	1852	10	7.1
D	6	6.1	326	69	0.21	0.364	3.245	0.026	0.11646	0.00059	3.257	0.026	0.11327	0.00083	1726	12	1853	13	6.8
D	15	15.1	217	48	0.22	0.218	4.389	0.038	0.11627	0.00071	4.399	0.038	0.11436	0.00087	1321	10	1870	14	29.4
D	4	4.1	381	174	0.46	0.224	2.809	0.021	0.13086	0.00048	2.815	0.021	0.12889	0.00059	1960	13	2083	8	5.9
D	16	16.1	193	111	0.57	0.042	2.116	0.019	0.18272	0.00077	2.117	0.019	0.18235	0.00079	2494	18	2674	7	6.7

The dates of 1747 and 1735 Ma for the two analyses in Group P are interpreted to reflect minor ancient radiogenic Pb loss.

References

Bagas, L, Bierlein, FP, Anderson, JAC and Maas, R 2010, Collision-related granitic magmatism in the Granites-Tanami Orogen, Western Australia: Precambrian Research, v. 177, p. 212–226.

Eacott, GR and de Souza Kovacs, N 2015, Lewis, WA Sheet 4567: Geological Survey of Western Australia, 1:100 000 Geological Series.

Lu, Y, Wingate, MTD and Maidment, DW 2018, 189936: biotite–hornblende granodiorite, Lewis Range; Geochronology Record 1511: Geological Survey of Western Australia, 4p.

Lu, Y, Wingate, MTD and Maidment, DW 2018b, 189937: biotite monzogranite, Lewis Range; Geochronology Record 1512: Geological Survey of Western Australia, 4p.

Stacey, JS, and Kramers, JD 1975, Approximation of terrestrial lead isotope evolution by a two-stage model: Earth and Planetary Science Letters, v. 26, p. 207–221.

Recommended reference for this publication

Lu, Y, Wingate, MTD and Maidment, DW 2018, 189942: muscovite–biotite syenogranite, Lewis Range; Geochronology Record 1513: Geological Survey of Western Australia, 4p.

Data obtained: 21 July 2008

Data released: 15 June 2018